Int J Clin Exp Pathol (2009) 2, 34-47
www.ijcep.com/IJCEP803012

Original Article

Decreased Survival and Hepato-Renal Pathology in Mice with C-Terminally Truncated GP73 (GOLPH2)

Lorinda Marie Wright[1, 2], Sheri Yong[3], Maria Mrozowicz Picken[3], Don Rockey[4] and Claus Jüergen Fimmel[1, 2]

[1]Division of Gastroenterology, Hepatology and Nutrition, Loyola University, Stritch School of Medicine, Maywood, IL, USA; [2]Edward Hines VA Medical Center, Hines, IL, USA; [3]Department of Pathology, Loyola University, Stritch School of Medicine, Maywood, IL, USA and [4]Internal Medicine, Digestive & Liver Diseases, UT Southwestern Medical Center, Dallas, TX, USA

Received 21 March 2008; Accepted with revision 14 April 2008; Available online 24 April 2008

Abstract: GP73 (Golph2) is a type II Golgi-localized integral membrane protein that is normally expressed in epithelial cells of many human tissues, and that is highly upregulated in liver disease. While its function is unknown, the GP73 C-terminus contains putative protein-interaction domains. We used a gene trap approach to generate mice with a severe truncation of the GP73 C-terminus ($GP73^{tr/tr}$) in order to investigate the physiological role of this protein. $GP73^{tr/tr}$ mice were born at the expected rate and were fertile, but cumulative survival was significantly reduced compared to wild-type controls, particularly in females. $GP73^{tr/tr}$ mice developed varying degrees of renal disease, most notably focal segmental glomerulosclerosis and hyaline thrombi. In addition to renal abnormalities, $GP73^{tr/tr}$ mice developed marked microvesicular hepatic steatosis, hepatocyte nuclear membrane irregularities and intranuclear inclusions. $GP73^{tr/tr}$ expression in morphologically normal kidneys and livers was constitutively low, but was strikingly upregulated in the diseased kidney cortex, and was upregulated in livers in animals of advanced age. Despite the substantial morphological changes in the kidneys and liver, routine screening serum assays provided no evidence of renal or hepatic dysfunction. Consequently, the cause of the increased mortality of $GP73^{tr/tr}$ animals is unclear at present. Our study indicates that GP73 is essential for normal survival, and suggests multiple roles for GP73 in epithelial cell function in the kidney and liver.
Key Words: GP73 (Golph2), epithelial cells, Golgi membrane protein, hyaline thrombi, glomerulosclerosis, hepatic steatosis

Introduction

We have previously reported the isolation and cloning of a novel Golgi-localized membrane protein, GP73, also known as Golgi phosphoprotein 2 (Golph2), or Golgi membrane protein 1 (Golm1). GP73 is widely expressed in normal epithelial cells from numerous tissues. Its function is unknown. GP73 expression is upregulated in hepatocytes of patients with acute and chronic liver disease [1, 2], regardless of the specific disease etiology. Resolution of hepatitis is paralleled by a reduction and normalization of GP73 expression, indicating that GP73 may be triggered by the hepatic injury response. A circulating form of GP73 is found in the serum of patients with hepatocellular cancer (HCC). These data indicate that serum GP73 is a promising diagnostic marker for liver cancer [3-5].

GP73 has a single short N-terminal transmembrane domain and a large C-terminal ectodomain that faces the Golgi lumen. The C-terminus contains a coiled-coil domain that is necessary for Golgi localization and retrieval to the *cis*-Golgi under steady-state conditions [6]. The C-terminus also contains a highly acidic domain of unknown function. GP73 cycles to the cell surface and is retrieved to the Golgi complex via late endosomes. Cleavage of the C-terminal ectodomain occurs via a proprotein convertase site, and results in its appearance in serum [7].

Based on its apparent role in liver disease, its potential utility as an HCC biomarker, and the

lack of an obvious function, we were interested in developing a transgenic mouse model of GP73 deficiency. We became aware of an existing embryonic stem cell line containing a large C-terminal truncation of the murine homolog of GP73. In this report, we describe the development of a mouse model with C-terminally truncated GP73 ($GP73^{tr/tr}$). The truncated protein lacks most of the C-terminal acidic domain, but retains its Golgi-targeting and proprotein convertase domains. Our data indicates that lack of full-length GP73 results in decreased survival and severe epithelial abnormalities of the kidney and the liver. Our findings suggest that GP73 plays important roles in epithelial cell function.

Materials and Methods

Transgenic Mice

All procedures were approved by the Institutional Animal Care and Use Committees at the Edward Hines Jr. VA Hospital, and at the University of Texas Southwestern. All animals received humane care according to the NIH Guide for the Care and Use of Laboratory Animals. Mice were fed a normal chow diet (Harlan Teklad Rodent Diet, Harlan Teklad, Madison, WI, USA), and maintained on a 12h light-dark cycle. The 129x1/Sv embryonic stem (ES) cell line KST273 (International Gene Trap Consortium, http://www.genetrap.org/contact/index.html) [8] containing the non-secretory gene trap vector, pGT1TMPFS inserted into the GP73 gene was used to generate $GP73^{tr/tr}$ mice. This vector consisted of the engrailed 2 (*En*-2) intron upstream of the gene encoding the β-galactosidase (β-gal)/neomycin-resistance fusion protein (*β-geo*) [9]. The KST273 ES cell line was injected into C57BL/6 blastocysts to create male chimeric mice. Mixed background C57BL/6J x 129x1/Sv mice were generated by mating male chimeras with wild-type C57BL/6J female mice (Jackson Laboratory, Bar Harbor, ME, USA), and intercrossing the resulting F1 heterozygous progeny. All experiments reported here were performed with F2 and subsequent generations of $GP73^{+/+}$ and $GP73^{tr/tr}$ mice of this mixed background maintained through sibling-matings.

Genotyping

DNA was prepared from tail snips by digestion with proteinase K (Amresco, Inc., Solon, OH, USA) at 55°C overnight, and PCR reactions were set up using an exon 8 forward primer (E8F; 5'-AGATTCAGGCTGTCGGTGAG-3') and an intron 8 reverse primer (I8R; 5'-GTCATATGAGGAGGCCTGGA-3') to amplify a 1044 bp region spanning the gene trap insertion site of the GP73 gene. Parallel reactions were set up using an intron 7 forward primer (I7F; 5'- CACTCACTGTGGAGGCAGAA-3') and a reverse primer specific for the 5' end of the insertion vector sequence (BGR; 5'-CCTGGCCTCCAGACAAGTAG-3') to amplify an 867 bp product present only in mice with a truncated GP73 allele. The 12,100 bp vector sequence in the mutated allele prevented the amplification of any product from the E8F/I8R primer pair. To amplify a 681 bp region of the β-gal product from the insert, forward (β-GalF; 5'-TTATCGATGAGCGTGGTGGTTATGC-3') and reverse (β-GalR; 5'-GCGCGTACATCGGGCAAATAATATC-3') primers were used. PCR reactions were run for 35 (E8F/I8R, I7F/BGR) or 32 (β-Gal) cycles with an annealing temperature of 63ºC, and products were visualized with ethidium bromide after electrophoresis through a 1.5% agarose gel. PCR products were sequenced at the Protein and Nucleic Acid Chemistry Laboratory at Washington University after amplification with either the specific forward or reverse primer and the ABI Prism BigDye Terminator Premix (Applied Biosystems, Foster City, CA, USA). Unincorporated dye and nucleotides were removed by centrifugation through EdgeBio Performa Spin Columns (EdgeBio Systems, Gaithersburg, MD, USA).

Southern Blotting

Mouse DNA purified from tail snips was restriction-digested overnight with *SphI* (New England Biolabs, Ipswich, MA, USA) to create either a 4376 bp fragment from the wild-type ($GP73^{+/+}$) allele or a 10,299 bp fragment from the $GP73^{tr/tr}$ allele. DNA (20 µg) was separated on a 0.7% agarose gel at 60V in Tris-acetate-EDTA (TAE, 0.04M Tris-base, 0.02M acetic acid, 0.001M EDTA), and transferred to positively charged nylon membrane (Zeta-Probe GT, Bio-Rad, Hercules, CA). A unique 1.1 kb region within intron 6 of the murine GP73 gene was PCR-amplified using forward primer 5'-GATCGACGTCTGATCTTATATATGTG-3' and reverse primer 5'-GATCGGGACCCTCATTAGTAAGTAAG-3'. The PCR fragment was digested with *SanDI*

(Stratagene, La Jolla, CA, USA) and *AatII* (New England Biolabs), subcloned into pBS-SK (+/-) (Invitrogen, Carlsbad, CA, USA) and used as a probe. Membranes were prehybridized for 4-6h at 66°C in hybridization buffer (9% dextran sulfate, 10x Denhardt's solution, 3x SSC, 0.5% SDS, and 100 µg/mL denatured salmon sperm DNA), then hybridized with the [^{32}P]dCTP-labeled probe overnight at 66ºC. Membranes were washed 4 times with 2X SSC, 0.1% SDS for 5 min at room temperature, and once with 0.1X SSC, 0.1% SDS at 65°C for 10 min and exposed to film at -70ºC.

RNA Isolation and Reverse Transcriptase Polymerase Chain Reaction (RT-PCR)

Mouse tissues were harvested immediately after euthanasia and snap frozen in liquid N_2. Total RNA was isolated using TRI Reagent (Molecular Research Center, Inc, Cincinnati, OH, USA) [10]. First strand cDNA synthesis was performed using 5 µg of total RNA and MLV-reverse transcriptase (Ambion, Austin, TX, USA) at 37°C for 50 min. Expression levels of GP73 mRNA were compared by semi-quantitative RT-PCR with specific forward and reverse primers designed to amplify a 181 bp region of exons 6 and 7 (E6/E7; 5'-CAGTGTGACGAGCGGATAGA-3' forward; 5'-ACTTGTTTCTGGGCACATCC-3' reverse) common to all mice regardless of genotype. RT-PCR reactions were run using 150 ng of RNA and the 'hot start' PCR method at 94°C for 30 sec, 61°C for 1 min, and 72°C for 1 min for 27 cycles. Parallel reactions were run using 200 ng of RNA and primers for amplification of GAPDH (T_{Anneal} = 60°C, 22 cycles) as described [11]. Products were visualized with ethidium bromide. Band intensities were quantified using Scion Image (Scion Corporation, Frederick, MD, USA), and GP73 levels expressed relative to GAPDH.

Histology

Mouse tissues were fixed in 10% formalin, paraffin embedded, sectioned, and stained with Hematoxylin and Eosin (H&E) according to standard methods by the Molecular Core Resource Facility in the Department of Pathology at Loyola University. Kidney sections were additionally stained with periodic acid/Schiff (PAS). Sections were viewed on a Zeiss Axiovert 200M inverted microscope and photographed. Image analysis of glomeruli was performed using the Scion Image program [12]. For β-gal staining, tissues were embedded in OCT (Ted Pella, Inc, Redding, CA), frozen in a dry ice/isopentane bath, and cryosectioned according to standard methods by the Molecular Core Resource Facility in the Department of Pathology at Loyola University. Cryosections were fixed for 10 min in 2% formaldehyde, 0.2% glutaraldehyde in phosphate buffered saline (PBS), washed several times in wash buffer (PBS, pH 7.3 containing 2 mM $MgCl_2$, 0.1% sodium deoxycholate, and 0.01% Nonidet P-40), then stained in wash buffer containing 5 mM $K_4Fe(CN)_6$-$3H_2O$, 5 mM $K_3Fe(CN)_6$ and 1 mM X-Gal (Invitrogen) at 37ºC for 1.5-24 h until the desired staining intensity was reached. Tissues were post-fixed overnight in 100 mM NaH_2PO_4, 67.5 mM NaOH, 3.7% formaldehyde, 1% glutaraldehyde, pH 7.2, then counterstained for 15 min in Hematoxylin (according to Mayer, Fluka, Buchs, Switzerland), and for 15 sec in Eosin Y (2.5% in H_2O, Sigma, St. Louis, MO). For Oil Red O staining cryosections were formalin-fixed for 10 min, rinsed briefly in isopropanol, and stained for 15 min in a 0.75% solution of Oil Red O (Sigma) in isopropanol. Sections were rinsed in isopropanol, and viewed on a Zeiss Axiovert 200M inverted microscope.

Induction of Liver Cirrhosis

To induce liver injury in adult $GP73^{+/+}$ male BALB/C mice, carbon tetrachloride (CCl_4) was mixed with corn oil (1:1) and given by gavage at 2.0ml/kg once weekly for 4 weeks as described [13]. Animals receiving corn oil alone served as controls.

Blood Chemistries

Approximately 1 mL of blood was drawn immediately post-euthanasia by cardiac puncture using a 22-gauge needle. Blood was placed into PST Tubes with lithium heparin (BD Biosciences, Sparks, MD, USA) and centrifuged at 10,000 x g for 10 min for serum separation. Serum was transported immediately to the Clinical Chemistry Department at the Edward Hines VA Hospital for analysis on an autoanalyzer according to standard techniques. Serum levels of cholesterol, triglycerides (Trig), aspartate aminotransferase (AST), alanine aminotransferase (ALT), lactate dehydrogenase (LDH), alkaline phosphatase

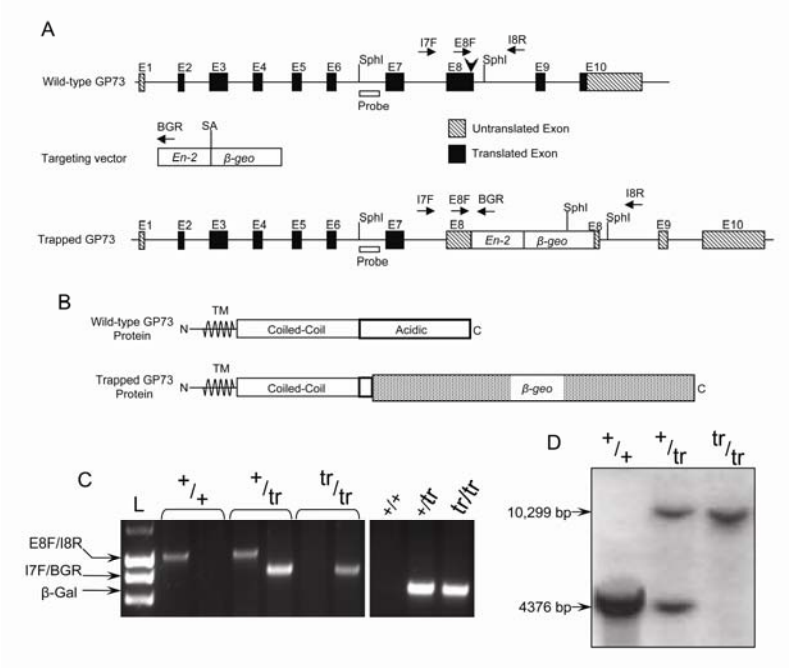

Figure 1 Generation of mice with a truncated GP73 gene. **A**. Top: Map of the wild-type mouse GP73 gene. *SphI* cleavage sites, vector insertion site (arrowhead), Southern probe, and genotyping primers (arrows) are indicated. Middle: The gene-trap targeting vector is depicted with the splice acceptor (SA) of the mouse *En-2* gene and the *β-geo* reporter sequences. *SphI* cleavage site and the reverse genotyping primer are indicated. Bottom: The mutant GP73 allele following insertion of the gene trap vector. **B**. Top: Predicted wild-type GP73 protein with the transmembrane domain (TM), and C-terminal coiled-coil and acidic domains shown. Bottom: Predicted GP73/β-Geo fusion protein with C-terminal truncation of GP73. **C**. Left: PCR genotyping of $GP73^{+/+}$ $GP73^{+/tr}$, and $GP73^{tr/tr}$ mice. Primer pairs used to generate each PCR product are indicated. Right: PCR-amplification of β-gal sequence from $GP73^{+/+}$, $GP73^{+/tr}$, and $GP73^{tr/tr}$ mice. **D**. Southern blot of $GP73^{+/+}$, $GP73^{+/tr}$, and $GP73^{tr/tr}$ mice. The 4376 bp fragment generated from the $GP73^{+/+}$ allele, and 10,299 bp fragment generated from the $GP73^{tr/tr}$ allele are indicated.

(ALP), creatinine, and glucose were determined.

Data Analysis

Results are presented as the mean ± standard error of the mean of at least three independent experiments. Differences between treatments were analyzed using single-factor ANOVA. The log rank test was used to calculate significance in Kaplan-Meier survival analyses. A *P* value of < 0.05 was considered significant.

Results

Characterization of $GP73^{tr/tr}$ Mice

The ES cell line KST273 (BayGenomics) contains a gene trap insertional mutation linked to a region of homology to GP73 exons 3-7. This construct was used to generate mice with a C-terminal truncation of the GP73 gene. The exact insertion site of the gene trap insert was determined by PCR genotyping using an intron 7 forward primer and a gene trap specific reverse primer. Sequencing of the PCR product demonstrated that the vector had inserted 6 bp 5' to the end of exon 8 (**Figure 1A**). In order to determine whether exon 8 was transcribed, we performed RT-PCR on gastric mRNA using an exon 7 forward primer (5'-ACCTGGCTGAAACCAACAAC-3') and a gene trap-specific reverse primer (5'-CACCACCAGGTTCACTTCCT-3'). Reactions were run for 35 cycles using an annealing temperature of 60ºC. Sequencing of the RT-PCR product demonstrated the loss of exon 8, indicating fusion of GP73 exon 7 to the insert *β-gal* gene. Based on this result, we used an exon 8 forward primer (E8F) and an intron 8 reverse primer (I8R) to test for the wild-type allele in PCR genotyping reactions. We used an intron 7 forward primer (I7F) and a gene trap specific reverse primer (BGR) to test for the

truncated allele (**Figure 1C**, left). Southern blotting of genomic DNA confirmed the insertion of the vector within exon 8 of *GP73* (**Figure 1D**). To show that the vector inserted only once, we performed PCR reactions using forward and reverse primers located within the *β-gal* exon. Out of 198 mice tested, every mouse positive for the *β-gal* sequence was also positive for the I7F/BGR product (**Figure 1C**, right), confirming a single vector insertion site within the GP73 gene. Thus, $GP73^{tr/tr}$ mice expressed a truncated version of GP73 lacking 146 residues of the C-terminus corresponding to 37% of the total protein and more than 70% of the C-terminal acidic ectodomain. The remaining protein retained the transmembrane domain, coiled-coil domain, and proprotein convertase site (**Figure 1B**).

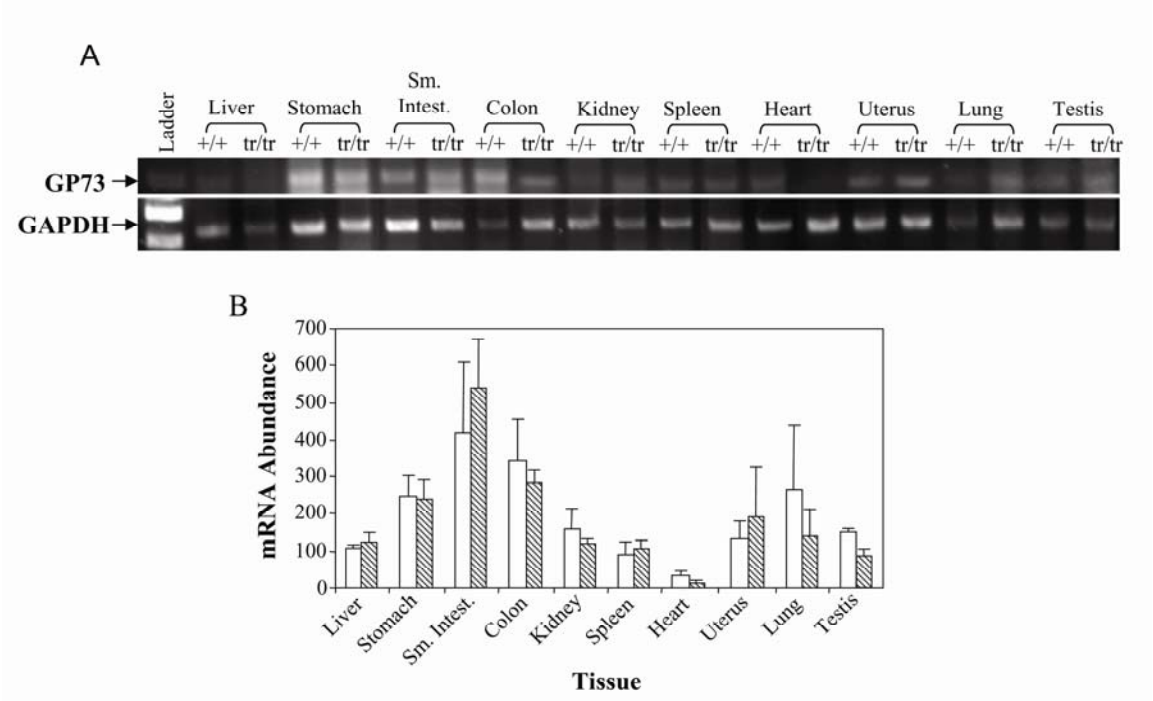

Figure 2 GP73 mRNA expression in $GP73^{+/+}$ and $GP73^{tr/tr}$ mouse tissues. **A**. RT-PCR of GP73 and GAPDH mRNA expression levels in indicated $GP73^{+/+}$, and $GP73^{tr/tr}$ tissues. RT-PCR was performed using the E6/E7 primer set to amplify exons 6 and 7 common to both $GP73^{+/+}$, and $GP73^{tr/tr}$ alleles. **B**. GAPDH-normalized band intensities of GP73 mRNA from $GP73^{+/+}$ (open bars) and $GP73^{tr/tr}$ (hatched bars) mice.

GP73 mRNA is Expressed in Epithelial Tissues

We measured GP73 mRNA levels in various tissues from $GP73^{+/+}$ and $GP73^{tr/tr}$ mice using primers that amplified a region of exons 6 and 7 common to both alleles (**Figure 2**). GP73 mRNA expression was highest in small intestine, colon, and stomach, while expression in the heart was minimal. Low, but detectable GP73 mRNA expression levels were found in liver, kidney, spleen, lung, uterus, and testis. Total GP73 mRNA levels in different tissues were similar for $GP73^{+/+}$ and $GP73^{tr/tr}$ mice (**Figure 2B**), indicating that transcriptional regulation of the $GP73^{tr/tr}$ allele was preserved.

$GP73^{tr/tr}$ Protein is Expressed in Epithelial Tissues

We used the *β-geo* reporter to detect the presence of the fusion protein in $GP73^{tr/tr}$ animals (**Figure 3**). β-gal staining was prominent in the columnar epithelium of gastric glands (**Figure 3A**). Similarly, the colon (**Figure 3B**) and small intestine (**Figure 3C**) showed robust β-gal staining of columnar epithelial cells on the lumenal surface of intestinal glands, particularly in the small intestine. Staining appeared in a punctate perinuclear pattern typical of a Golgi localization. Staining was typically more

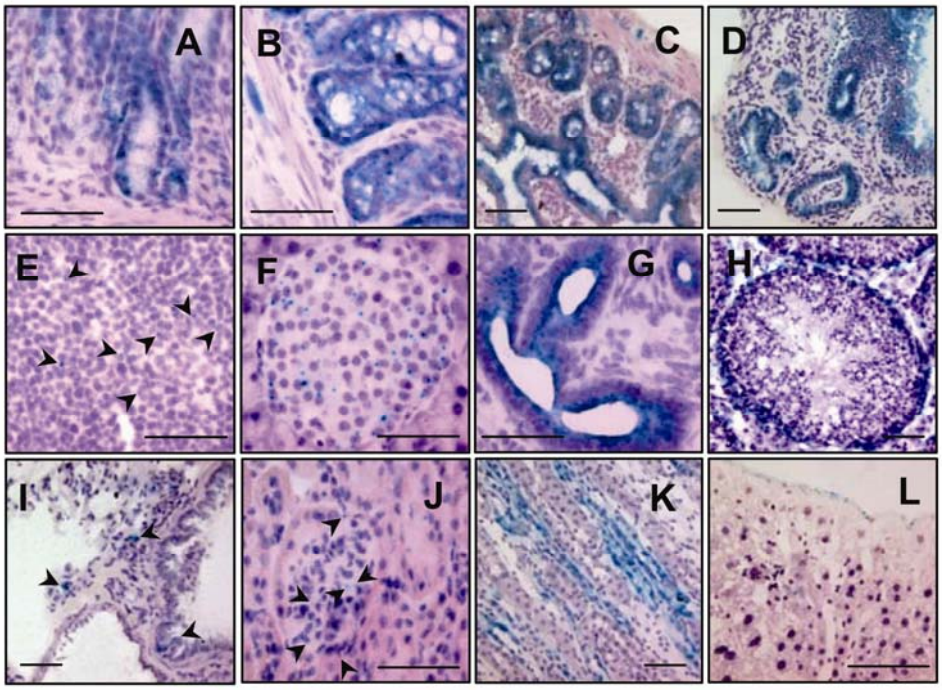

Figure 3 The GP73/β-*geo* fusion protein is predominantly expressed in epithelial cells. Cryosections were stained for β-gal expression (light blue, *arrowheads*), and counterstained with Eosin Y and hematoxylin (purple). Photomicrographs of stomach (**A**), colon (**B**), small intestine (**C**), gall bladder (**D**), spleen (**E**), pancreas (**F**), uterus (**G**), testis (**H**), lung (**I**), kidney cortex (**J**), kidney medulla (**K**), and liver (**L**) from $GP73^{tr/tr}$ mice. Bars = 50 μm.

intense in the base of the glands, and decreased in the apical portion of intestinal glands. Columnar epithelial cells of the gallbladder mucosa also stained positive (**Figure 3D**). The spleen (**Figure 3E**) showed rare, positive cells exclusively within the white pulp. Expression in the pancreas (**Figure 3F**) was found only within islet cells. The uterus (**Figure 3G**) showed strong staining in endometrial epithelial cells. Expression in the testis (**Figure 3H**) was limited to germ cells or Sertoli cells. The lungs (**Figure 3I**) showed occasional expression in columnar respiratory epithelial cells. Within the kidney cortex, rare positive cells were localized to glomerular capillaries and Bowman's capsules (**Figure 3J**). In the medulla, stronger staining was present in collecting tubules (**Figure 3K**). In the liver, staining was limited to mesothelial cells within the Glisson's capsule, whereas hepatocytes were universally negative (**Figure 3L**).

Reduced Survival in $GP73^{tr/tr}$ Mice

Matings between heterozygous mice produced the expected distribution of $GP73^{+/+}$, $GP73^{+/tr}$ and $GP73^{tr/tr}$ pups, and male and female $GP73^{tr/tr}$ mice had growth rates and adult weights similar to $GP73^{+/+}$ controls (data not shown). However, life table analysis of 64 $GP73^{+/+}$ males, 81 $GP73^{+/+}$ females, 102 $GP73^{tr/tr}$ males, and 121 $GP73^{tr/tr}$ females demonstrated a progressive decrease in survival in $GP73^{tr/tr}$ mice that was particularly pronounced in females (**Figure 4**). This reduction in survival began to be apparent at 3 weeks of age. At 18 months survival in $GP73^{tr/tr}$ males was reduced to 86.7% compared to 100% survival in $GP73^{+/+}$ males ($P = 0.0153$). Survival in $GP73^{tr/tr}$ females was markedly reduced to 50.8% compared to 79.7% in $GP73^{+/+}$ females ($P = 0.0232$).

Renal Disease in $GP73^{tr/tr}$ Mice

Death in $GP73^{tr/tr}$ mice was typically preceded by a 3 week period of moderate weight loss, rough coat, and lethargy. Necropsy of $GP73^{tr/tr}$ mice that were euthanized prematurely because of these symptoms of illness commonly revealed markedly pale and atrophic kidneys with macroscopically visible casts(**Figure 5B**). In comparison, the kidneys of $GP73^{+/+}$ mice had a normal gross appearance (**Figure 5B**). All other organs had a normal gross appearance upon necropsy, and no

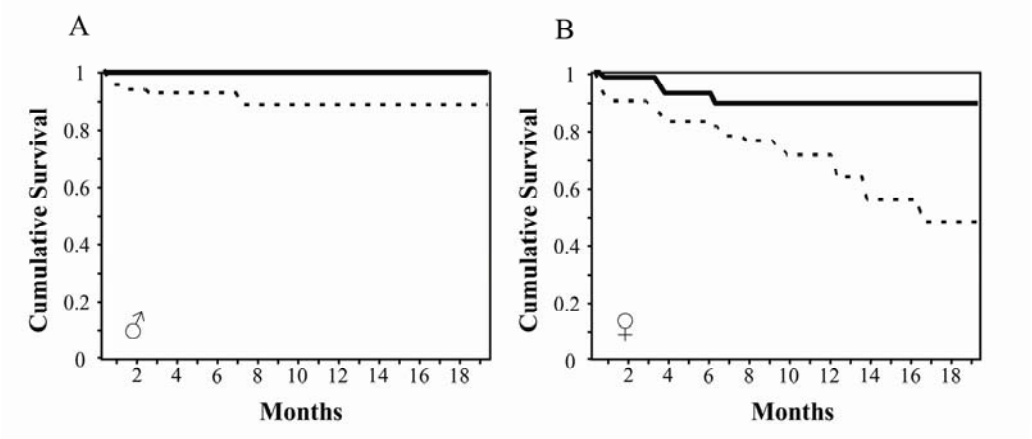

Figure 4 Decreased survival in GP73$^{tr/tr}$ mice. Kaplan-Meier plots of cumulative survival of GP73$^{+/+}$ (solid line) and GP73$^{tr/tr}$ (dotted line) male (**A**) and female (**B**) mice.

significant differences in wet weights of lung, liver, heart, small intestine, colon, stomach, or pancreas were found between wild-type and GP73$^{tr/tr}$ animals (data not shown). Microscopically, the abnormal kidneys of GP73$^{tr/tr}$ mice displayed widespread glomerulosclerosis and intratubular casts (**Figure 5B**) compared to the normal renal histology in GP73$^{+/+}$ animals (**Figure 5C**).

Similar but less marked abnormalities were also noted in GP73$^{tr/tr}$ mice that exhibited no disease symptoms prior to euthanasia. Detailed analysis of these changes revealed subtle, gender-dependent differences. The majority of female GP73$^{tr/tr}$ mice developed focal segmental glomerulosclerosis (FSGS), and PAS-positive glomerular hyaline thrombi were more commonly seen in female than male animals (40% vs 15%; **Figure 5E**). Similarly, inflammatory cell infiltrates at the cortical-medullary junction were present more frequently in female animals than in males (40% vs 19%; **Figure 5H**). Conversely, degenerative changes in proximal tubules (**Figure 5F**) appeared more prominent in male animals than females (75% vs 12.5%). Finally, some abnormalities were observed at similar frequencies in both genders, including glomerular hypertrophy – a finding that is suggestive of nephron loss (**Figure 5G**), and fibrotic thickening of Bowman's capsules.

Regardless of their gender distribution, the histological abnormalities in the kidneys increased in frequency with the animals' age, resulting in the presence of some degree of renal pathology in approximately 90% of all GP73$^{tr/tr}$ mice by the age of six months.

Despite these extensive histological abnormalities, we were unable to detect any significant differences in serum creatinine and glucose concentrations between GP73$^{+/+}$ and GP73$^{tr/tr}$ mice (data not shown), suggesting that glomerular filtration was preserved in GP73$^{tr/tr}$ mice.

Steatohepatitis in GP73$^{tr/tr}$ Livers

GP73$^{tr/tr}$ male and female mice developed microvesicular (**Figure 6B**) and mixed pattern (**Figure 6C**) hepatic steatosis. In contrast, the livers of wild-type animals were histologically normal (**Figure 6A**). Hepatic steatosis in GP73$^{tr/tr}$ animals occurred while the animals were fed a regular chow diet. We considered the possibility that hepatic steatosis might be due to obesity. Interestingly, mean age-matched adult body weights were no different in GP73$^{tr/tr}$ animals compared to wild-type controls. Furthermore, we analyzed the liver histologies of normal-weight, gender- and weight-matched wild-type and GP73$^{tr/tr}$ animals. Normal-weight, wild-type mice had only occasional lipid accumulations detected by Oil Red O staining (**Figure 6D**). In contrast, marked steatosis was present in GP73$^{tr/tr}$ animals (**Figure 6E**). The distribution of hepatic steatosis was central-lobular and mid-zonal, and became panlobular in the most severe cases (**Figure 6F**). In addition, lobular and periportal inflammation was frequently observed in the livers of GP73$^{tr/tr}$ animals (**Figure 6G**).

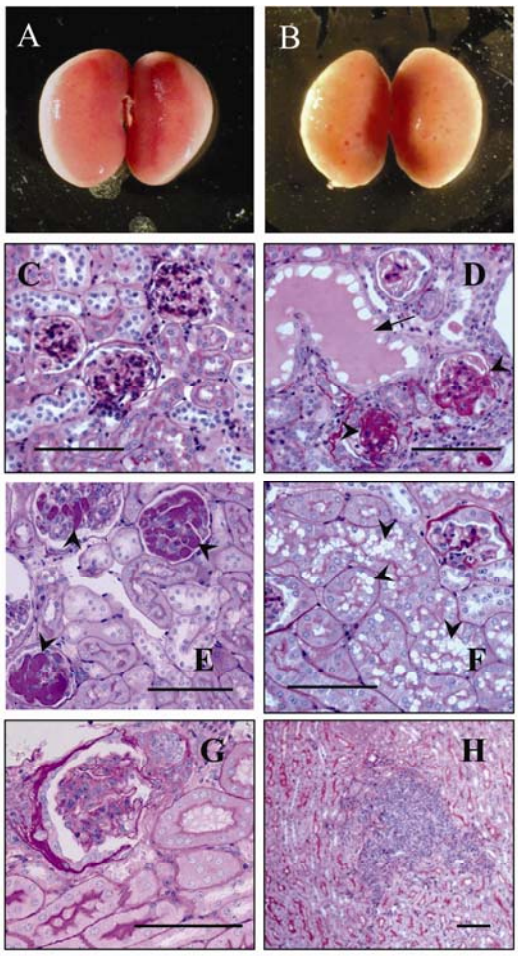

Figure 5 Renal abnormalities in GP73$^{tr/tr}$ mice. Whole kidneys from GP73$^{+/+}$ (**A**), and GP73$^{tr/tr}$ (**B**) mice. Photomicrographs of kidney sections from GP73$^{+/+}$ (**C**), and GP73$^{tr/tr}$ (**D**-**H**) mice stained with H&E and PAS. GP73$^{tr/tr}$ mice developed glomerulosclerosis (arrowheads) and intratubular casts (*arrowhead,* **D**), formation of PAS-positive hyaline thrombi (arrowheads, **E**), degenerative changes in proximal collecting tubules (arrowheads, **F**), glomerular hypertrophy and thickening of Bowman's capsule (**G**), and collections of lymphocytes at the cortical-medullary junction (**H**), bars = 100 µm.

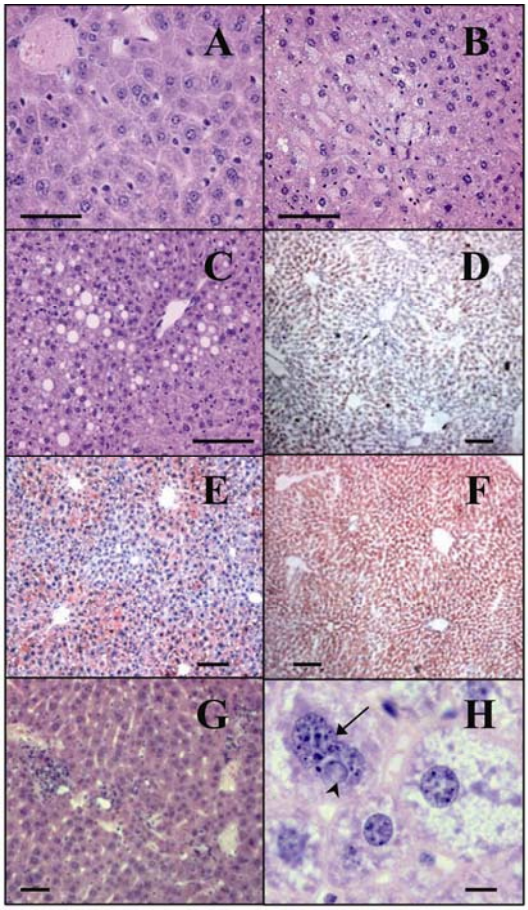

Figure 6 Steatosis and lobular inflammation in GP73$^{tr/tr}$ livers. Compared to normal livers from GP73$^{+/+}$ mice (**A**), livers from male and female GP73$^{tr/tr}$ mice of average adult weight (31g) frequently showed extensive microvesicular (**B**) and mixed pattern (**C**) steatosis, bars = 50 µm. Oil Red O staining revealed extensive lipid accumulation in GP73$^{tr/tr}$ mice (**E** and **F**) compared to weight-matched GP73$^{+/+}$ controls (**D**), bars = 100 µm. Lobular inflammatory infiltrates were also common findings (**G**), bar = 50 µm. Male and female GP73$^{tr/tr}$ livers showed nuclei with circumferential membrane irregularities (arrow), and intranuclear inclusions (arrowhead, **H**). Microvesicular steatosis was also apparent, bar = 10 µm.

High-power views of individual hepatocytes revealed marked membrane irregularities and intranuclear inclusions in GP73$^{tr/tr}$ animals (**Figure 6H**). Despite the striking histological alterations in liver histology, we found no differences in the serum levels of cholesterol, Trig, ALP, AST, ALT, or LDH between wild-type and GP73$^{tr/tr}$ mice (data not shown), suggesting that overall liver function was not significantly altered.

Upregulation of GP73$^{tr/tr}$ mRNA and Protein Expression in Kidney and Liver Tissues

We used β-gal staining to analyze the cellular expression of the truncated GP73 protein in kidneys with glomerulosclerosis and hyaline thrombi accumulation. Increased expression of the GP73$^{tr/tr}$ protein was seen in cortical proximal tubules (**Figure 7A**), and in the Bowman's capsule and glomerular epithelial cells (**Figure 7B**). Hyaline thrombi were β-gal

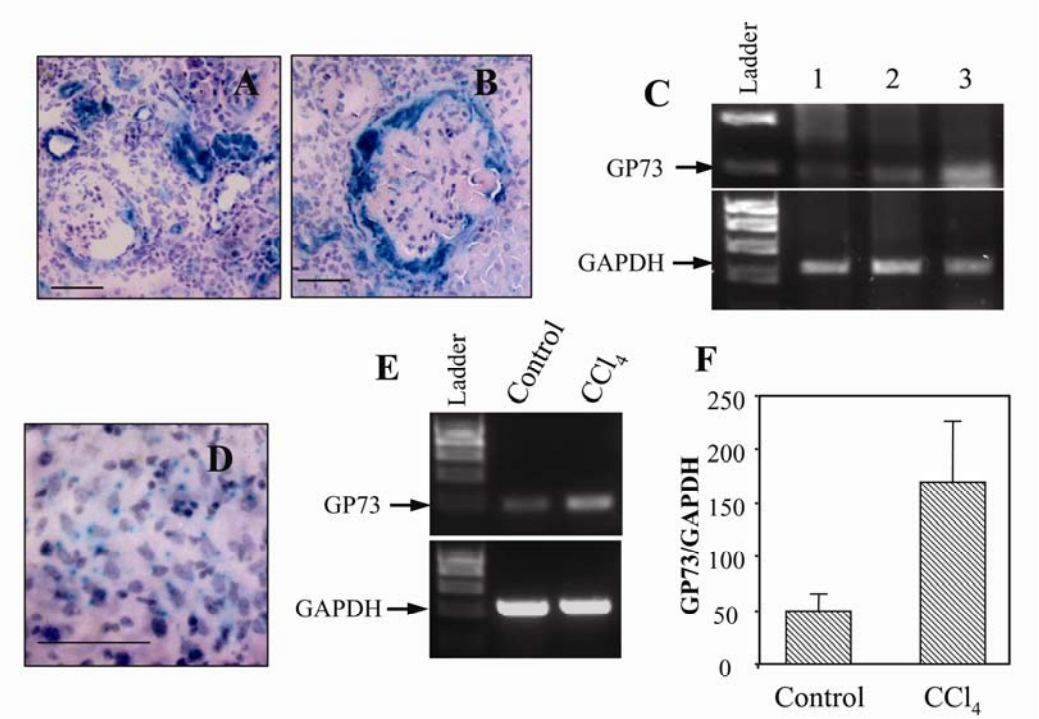

Figure 7 Renal and hepatic abnormalities are associated with upregulated GP73 expression. GP73/*β-Geo* staining in collecting tubules (**A**) and in Bowman's capsule of a kidney with hyaline thrombi (**B**), bars = 50 μm. RT-PCR analysis of GP73 mRNA levels from $GP73^{+/+}$ mice (1), $GP73^{tr/tr}$ mice without renal disease (2), and $GP73^{tr/tr}$ mice with renal damage (3) (**C**). GP73/*β-Geo* staining in hepatocytes of a $GP73^{tr/tr}$ mouse with nuclear abnormalities (**D**), bar = 50 μm. RT-PCR of GP73 mRNA expression from livers of $GP73^{+/+}$ mice treated with vehicle (control) or CCl_4. (**E**, **F**) GP73 mRNA levels from control and CCl_4-treated livers.

negative, indicating that they did not represent extracellular accumulations of $GP73^{tr/tr}$ protein. RT-PCR analysis confirmed the upregulation of $GP73^{tr/tr}$ mRNA at the whole-organ level (**Figure 7C**).

Similar studies performed on liver tissues suggested that the hepatocyte nuclear membrane abnormalities and hepatic steatosis in $GP73^{tr/tr}$ mice were not associated with upregulated $GP73^{tr/tr}$ expression. However, positive β-gal staining in hepatocytes was observed in older (≥ 18 months) $GP73^{tr/tr}$ mice (**Figure 7D**).

In order to assess whether the expression of wild-type GP73 was increased in more severe forms of liver disease, we examined GP73 mRNA levels in a mouse model of carbon tetrachloride (CCl_4)-induced cirrhosis. RT-PCR analysis revealed an approximately three-fold increase in GP73 mRNA levels in CCl_4-treated as compared to control livers (**Figures 7E** and **7F**). These data suggests that the upregulation of GP73 expression is a feature of severe murine liver disease, similar to our previous observations in human liver disease.

Discussion

GP73 is a resident membrane protein of the early (*cis-)* Golgi complex that is preferentially expressed in many normal human epithelial cells. We first identified GP73 based on its overexpression in the livers of patients with acute giant-cell hepatitis, and have since studied its role in different forms of human liver disease [1]. Hepatocyte expression of GP73 - normally absent or minimal – is dramatically upregulated in patients with acute and chronic hepatitis, liver cirrhosis, and hepatocellular cancer [2, 14]. The disease-related upregulation of GP73 is unusual, since the majority of known Golgi membrane proteins are constitutively expressed and not known to be regulated in response to disease processes. Many Golgi membrane proteins are involved in intracellular trafficking processes or in protein and lipid modification reactions. The dynamic regulation of GP73 suggests that this protein

may have unique biologic properties.

The function of GP73 is currently unclear, and sequence analysis algorithms have so far not revealed any suggestive motifs. However, we have elucidated unusual intracellular trafficking properties of GP73 in which some structural domains play crucial roles. Despite its steady-state localization to the *cis*-Golgi, GP73 normally cycles to the cell surface, and is retrieved to the Golgi complex via late endosomes. Correct retrieval is dependent on the coiled-coil domain located immediately C-terminal to the transmembrane domain [6]. Coiled-coil domains are known to be involved in protein-protein interactions, and such interactions may be necessary for GP73 retrieval [15, 16]. However, we have thus far been unable to identify proteins that specifically interact with this domain.

A circulating form of GP73 is present in the serum of patients with hepatocellular cancer [3, 4]. The cycling of GP73 to the cell membrane provides a mechanism whereby this Golgi-localized protein enters the serum. GP73 is released to the extracellular space from the cell membrane by cleavage of its luminal ectodomain by the proprotein convertase, furin [7]. The furin recognition site is located within the coiled-coil domain, 16 residues C-terminal to the membrane-spanning domain of the molecule. Thus, the C-terminal ectodomain that is released into the serum represents 87% of the total protein.

Less is known about the function of the acidic C-terminal domain of GP73. It has been speculated that acidic luminal domains of membrane proteins are involved in regulation of binding with charged proteins or ions [16], but this possibility has not been experimentally tested in this case.

GP73 sequences and its key domain features are highly conserved among mammals. The murine GP73 shares 63% amino acid identity with its human counterpart, and retains the domain features of the human protein. We reasoned that a murine GP73 mutant might result in informative phenotypic changes, and allow us to generate new hypotheses regarding the biologic function of the protein.

In the process of our studies, we became aware of an ES cell line (KST273) that contained a GP73-targeted gene trap insertional mutation. This cell line was developed by BayGenomics in a program designed to systematically mutate or inactivate all known or predicted transmembrane protein genes in the mouse. The gene trap vector acts as an artificial intron that overrides the intron splice donor/acceptor sites of the native gene. The translation of the native gene ends at the insertion site, and the N-terminus of the native gene is fused in-frame to a β-*geo* gene reporter sequence that allows the detection of the new fusion protein. ES cell lines developed through this project are part of the International Gene Trap Consortium and are public resources [8, 9].

We identified the exact insertion site of the KST273 vector within the GP73 gene, and characterized the mRNA sequence of the corresponding GP73 fusion gene. We determined that the KST273 vector inserts 6 bp prior to the end of exon 8 of GP73. Because exon 8 is interrupted, this insertion results in the loss of transcription of exon 8 and all downstream exons. The truncated gene retains the normal N-terminus, the single transmembrane domain, and the coiled-coil domain with the proprotein convertase site. The $GP73^{tr/tr}$ fusion protein lacks 146 C-terminal amino acids of the native protein, corresponding to 75% of the acidic luminal domain, and 37% of the total protein. β-Gal staining data indicates that the fusion protein exhibits a typical Golgi localization pattern, suggesting that its intracellular targeting remains intact (see **Figures 3** and **7**). Tissue expression patterns of $GP73^{tr/tr}$ in the mouse are substantially similar to those in humans [1], as well as published data on mouse GP73 (http://symatlas.gnf.org), further supporting the utility of this transgenic mouse as a model for human GP73 function. $GP73^{tr/tr}$ mRNA levels were similar to those of GP73 wild-type mRNA, indicating that the fusion gene retains its transcriptional regulation.

Our studies to date reveal that the truncation of the GP73 C-terminus results in pathological changes in the kidney and liver. Furthermore, $GP73^{tr/tr}$ mice have significantly reduced survival rates, although we do not know at present whether this effect is mediated by the renal and hepatic abnormalities observed. Finally, our data indicates a strong gender effect on the observed phenotype, since female mice had more severe renal pathologies and substantially higher mortality

rates than males.

The development of focal segmental glomerulosclerosis (FSGS) represents the most striking pathological renal alteration in GP73$^{tr/tr}$ mice. Based on human FSGS, a number of alternative pathways can be envisioned that might result in the observed changes. FSGS is observed in lymphoproliferative disorders such as non-Hodgkin lymphoma, multiple myeloma, and lymphoproliferative disorders [17-19], and in autoimmune diseases such as systemic lupus erythematosus [20, 21]. The abnormal proliferation of B-cell clones in these disorders leads to the overproduction of monoclonal IgM, which preferentially precipitates in the glomerular capillaries and leads to glomerulosclerosis [22]. We are planning to perform immunological studies to test these possibilities.

FSGS is typically associated with damage to glomerular podocytes, the capillary epithelial cells that play a key role in the regulation of glomerular filtration [23-25]. Our finding that GP73$^{tr/tr}$ is abnormally expressed in glomerular epithelial cells of animals with renal pathology suggests that podocyte expression of GP73 may be involved in the renal abnormalities of the mice [26].

Another striking morphological alteration in GP73$^{tr/tr}$ mice was the extensive deposition of hyaline thrombi in renal capillaries. Importantly, these deposits did not stain positively for β-gal even though intense β-gal activity was observed in the surrounding Bowman's capsules within the same sections. This result indicates that the glycoprotein deposits within the hyaline thrombi were not due to the release and accumulation of the abnormal GP73 fusion protein, and suggests that pathological changes in the kidneys of GP73$^{tr/tr}$ animals are not due to mistargeting of the fusion protein.

Histological studies of the liver revealed microvesicular hepatic steatosis and subtle steatohepatitis in the GP73$^{tr/tr}$ animals. The microvesicular fat globules often filled the cytoplasm of hepatocytes, but did not displace the nucleus. Similar changes can be seen in human fatty liver disease of pregnancy or in Reye's syndrome [27], two disorders associated with mitochondrial dysfunction and abnormal β-oxidation. It will be important to determine whether mitochondrial function is abnormal in GP73$^{tr/tr}$ animals.

Interestingly, the histological changes in the liver occurred even though hepatocyte expression of GP73$^{tr/tr}$ was undetectable in all but the oldest mice. It remains to be seen whether hepatic abnormalities are a direct result of the lack of normal GP73 function or an aberrant function of the truncated protein in hepatocytes, or whether the liver abnormalities are caused by as yet unknown extrahepatic metabolic changes or disease processes. The low hepatocyte expression of GP73 was reminiscent of a similar pattern in normal human livers [1]. Our observation of upregulated GP73 mRNA expression in the livers of animals with carbon tetrachloride-induced cirrhosis indicates that the murine GP73 is induced in the setting of severe liver disease. This finding is similar to the situation in human liver, where GP73 is dramatically upregulated in response to hepatic injury [1, 2, 14].

Of note, we found no morphological changes or histological evidence of disease in many organs that constitutively express GP73 at high levels, including the stomach, intestine, gall bladder, lung, uterus or testis. These data indicates that the lack of full-length GP73 expression does not affect the development or function of these epithelial tissues.

Nuclear membrane disruption and intranuclear inclusions were frequently observed in hepatocytes of GP73$^{tr/tr}$ mice. The nuclear membrane alterations in GP73$^{tr/tr}$ mice were frequently associated with elevated levels of steatosis, and tended to be more prominent in older GP73$^{tr/tr}$ mice. Since nuclear atypia is a feature of hepatocellular cancer, our findings raise the possibility that hepatic carcinogenesis may be increased in the GP73$^{tr/tr}$ mice [28, 29]. However, it remains to be established whether these nuclear changes are causally related to the hepatic phenotype, since similar changes have been previously reported in a variety of other transgenic mouse models [30, 31]. Studies to address these questions are currently under way in our laboratory.

Perhaps the most striking observation of our studies is the increased mortality of GP73$^{tr/tr}$ mice, especially in female animals. Although premature death in GP73$^{tr/tr}$ mice was associated with more severe hepatic and renal abnormalities compared to their surviving littermates, we can not be certain of the cause of death in these animals. Our preliminary

studies of serum chemistries did not provide any evidence for renal or hepatic failure, raising the possibility that as yet undiscovered alterations within these or other organs might be responsible for the increased mortality of the GP73$^{tr/tr}$ animals.

Finally, our studies indicate that the phenotypic changes observed in GP73$^{tr/tr}$ animals are gender-dependent. This observation is reminiscent of similar work with α-fetoprotein (AFP), a structurally unrelated protein with increased expression in hepatocellular cancer cells. AFP deficiency results in infertility of female mice, an unexpected phenotypic alteration that may be related to impaired sex hormone trafficking [32]. Our results suggest that GP73 expression is under hormonal control. Interestingly, others have previously shown that GP73 mRNA levels are modulated by estrogens and calcitriol [33, 34], a possibility that we are currently exploring.

We recognize two limitations of our model. First, we used a gene truncation rather than a null mutation. The expression of a Golgi-targeted truncation mutation might result in phenotypic changes that may not occur with a null mutant. Second, the GP73 truncation was global. Given the widespread expression of the wild-type protein, we consider the possibility that the observed changes in apparent target organs such as kidney and liver may be due to remote effects in other tissues. Ultimately, these limitations will only be overcome with the generation of tissue-specific null mutants of GP73. Nevertheless, our study provides intriguing evidence for an important role of GP73 in renal and hepatic function. The GP73$^{tr/tr}$ mouse model will allow us to test the role of this protein in experimentally induced renal and liver injury and hepato-carcinogenesis.

In summary, our study provides the first evidence for a critical role of the murine GP73 homolog for overall survival and the integrity of renal and hepatic tissues. Our findings suggest that the acidic C-terminus of the molecule may be required for normal GP73 function. The histological changes observed in GP73$^{tr/tr}$ livers and kidneys provide a rationale for future studies designed to test the immune system, renal and liver function, and hepatic carcinogenesis of GP73-deficient mice.

Acknowledgements

We thank Deborah Magnuson and Linda McKann for their excellent technical assistance, Michael Rauchman for directing us to the International Gene Trap Consortium database, and Susan Kiefer for introducing us to the basics of mouse transgenic work. This work was supported by funding from a VA Merit Review to C.J.F.

Please address all correspondences to Lorinda M. Wright, Ph.D., Division of Gastroenterology, Hepatology and Nutrition, Loyola University, Stritch School of Medicine, 2160 South 1st Avenue, Maywood, IL 60153, USA. Tel: 708-202-5717; Fax: 708-216-4113; Email: LMWright@LUMC.edu.

References

[1] Kladney RD, Bulla GA, Guo L, Mason AL, Tollefson AE, Simon DJ, Koutoubi Z and Fimmel CJ. GP73, a novel Golgi-localized protein upregulated by viral infection. *Gene* 2000;249: 53-65.

[2] Iftikhar R, Kladney RD, Havlioglu N, Schmitt-Graff A, Gusmirovic I, Solomon H, Luxon BA, Bacon BR and Fimmel CJ. Disease- and cell-specific expression of GP73 in human liver disease. *Am J Gastroenterol* 2004;99: 1087-1095.

[3] Block TM, Comunale MA, Lowman M, Steel LF, Romano PR, Fimmel C, Tennant BC, London WT, Evans AA, Blumberg BS, Dwek RA, Mattu TS and Mehta AS. Use of targeted glycoproteomics to identify serum glycoproteins that correlate with liver cancer in woodchucks and humans. *Proc Natl Acad Sci USA* 2005;102:779-784.

[4] Marrero JA, Romano PR, Nikolaeva O, Steel L, Mehta A, Fimmel CJ, Comunale MA, D'Amelio A, Lok AS and Block TM. GP73, a resident Golgi glycoprotein, is a novel serum marker for hepatocellular carcinoma. *J Hepatol* 2005;43: 1007-1012.

[5] Marrero JA and Lok AS. Newer markers for hepatocellular carcinoma. *Gastroenterology* 2004;127:S113-S119.

[6] Puri S, Bachert C, Fimmel CJ and Linstedt AD. Cycling of early Golgi proteins via the cell surface and endosomes upon lumenal pH disruption. *Traffic* 2002;3:641-653.

[7] Bachert C, Fimmel C and Linstedt AD. Endosomal trafficking and proprotein convertase cleavage of cis Golgi protein GP73 produces marker for hepatocellular carcinoma. *Traffic* 2007;8:1415-1423.

[8] Nord AS, Chang PJ, Conklin BR, Cox AV, Harper CA, Hicks GG, Huang CC, Johns SJ, Kawamoto M, Liu S, Meng EC, Morris JH, Rossant J, Ruiz P, Skarnes WC, Soriano P, Stanford WL, Stryke D, von Melchner H, Wurst W, Yamamura K, Young SG, Babbitt PC and Ferrin TE. The International Gene Trap Consortium website: A portal to all

publicly available gene trap cell lines in mouse. *Nucleic Acids Res* 2006;34:D642-D648.
[9] Stryke D, Kawamoto M, Huang CC, Johns SJ, King LA, Harper CA, Meng EC, Lee RE, Yee A, L'Italien L, Chuang PT, Young SG, Skarnes WC, Babbitt PC and Ferrin TE. BayGenomics: a resource of insertional mutations in mouse embryonic stem cells. *Nucleic Acids Res* 2003; 31:278-281.
[10] Chomczynski P and Sacchi N. Single step method of RNA isolation by an acid guanidinium thiocyanate-phenol-chloroform extraction. *Anal Biochem* 1987;162:156-159.
[11]Sunyer T, Lewis J, Collin-Osdoby P and Osdoby P. Estrogen's bone-protective effects may involve differential IL-1 receptor regulation in human osteoclast-like cells. *J Clin Invest* 1999;103: 1409-1418.
[12] Looi LM and Loh KC. Microwave-stimulated formaldehyde fixation of experimental renal biopsy tissues: Computerized morphometric analysis of distortion artifacts. *Malays J Pathol* 2005;27:23-27.
[13]Yata Y, Gotwals P, Koteliansky V and Rockey DC. Dose-dependent inhibition of hepatic fibrosis in mice by a TGF-beta soluble receptor: implications for antifibrotic therapy. *Hepatology (Baltimore, Md)* 2002;35:1022-1030.
[14] Kladney RD, Cui X, Bulla GA, Brunt EM and Fimmel CJ. Expression of GP73, a resident Golgi membrane protein, in viral and nonviral liver disease. *Hepatology (Baltimore, MD)* 2002;35:1431-1440.
[15]Wang C, Ivanov A, Chen L, Fredericks WJ, Seto E, Rauscher FJ, 3rd and Chen J. MDM2 interaction with nuclear corepressor KAP1 contributes to p53 inactivation. *EMBO J* 2005;24:3279-3290.
[16] Beard M, Satoh A, Shorter J and Warren G. A cryptic Rab1-binding site in the p115 tethering protein. *J Biol Chem* 2005;280:25840-25848.
[17] Chen R, Matthews JH and Jackson AC. Large granular lymphoproliferative disease associated with nephrotic syndrome, renal failure and leukoencephalopathy. *Leuk Lymphoma* 1993;11:129-133.
[18] Calvo Villas JM, Morales Umpierrez A, Ramirez Sanchez MJ and Cuesta Tovar J. Focal and segmental glomerulosclerosis and non-Hodgkin's lymphoma. *Clin Nephrol* 2002; 57:173-174.
[19] Shah S, Cavenagh J, Sheaf M and Thuraisingham RC. Remission of collapsing focal segmental glomerulosclerosis following chemotherapy for myeloma. *Am J Kidney Dis* 2004;43:e10-12.
[20] Jacob CO, Pricop L, Putterman C, Koss MN, Liu Y, Kollaros M, Bixler SA, Ambrose CM, Scott ML and Stohl W. Paucity of clinical disease despite serological autoimmunity and kidney pathology in lupus-prone New Zealand mixed 2328 mice deficient in BAFF. *J Immunol* 2006;177: 2671-2680.
[21] Mason LJ, Ravirajan CT, Latchman DS and Isenberg DA. A human anti-dsDNA monoclonal antibody caused hyaline thrombi formation in kidneys of 'leaky' SCID mice. *Clin Exp Immunol* 2001;126:137-142.
[22] Daghestani L and Pomeroy C. Renal manifestations of hepatitis C infection. *Am J Med* 1999;106:347-354.
[23] Wharram BL, Goyal M, Wiggins JE, Sanden SK, Hussain S, Filipiak WE, Saunders TL, Dysko RC, Kohno K, Holzman LB and Wiggins RC. Podocyte depletion causes glomerulosclerosis: Diphtheria toxin-induced podocyte depletion in rats expressing human diphtheria toxin receptor transgene. *J Am Soc Nephrol* 2005; 16:2941-2952.
[24] Kretzler M. Role of podocytes in focal sclerosis: Defining the point of no return. *J Am Soc Nephrol* 2005;16:2830-2832.
[25] Kretzler M, Koeppen-Hagemann I and Kriz W. Podocyte damage is a critical step in the development of glomerulosclerosis in the uninephrectomised-desoxycorticosterone hypertensive rat. *Virchows Arch* 1994;425: 181-193.
[26] Wiggins JE, Goyal M, Sanden SK, Wharram BL, Shedden KA, Misek DE, Kuick RD and Wiggins RC. Podocyte hypertrophy, "adaptation," and "decompensation" associated with glomerular enlargement and glomerulosclerosis in the aging rat: prevention by calorie restriction. *J Am Soc Nephrol* 2005;16:2953-2966.
[27] Badizadegan K and Perez-Atayde AR. Focal glycogenosis of the liver in disorders of ureagenesis: Its occurrence and diagnostic significance. *Hepatology (Baltimore, MD)* 1997;26:365-373.
[28] Quaglia A, Jutand MA, Dhillon A, Godfrey A, Togni R, Bioulac-Sage P, Balabaud C, Winnock M and Dhillon AP. Classification tool for the systematic histological assessment of hepatocellular carcinoma, macroregenerative nodules, and dysplastic nodules in cirrhotic liver. *World J Gastroenterol* 2005;11:6262-6268.
[29] Soyuer I, Ekinci C, Kaya M, Genc Y and Bahar K. Diagnosis of hepatocellular carcinoma by fine needle aspiration cytology. Cellular features. *Acta Cytol* 2003;47:581-589.
[30]Abel A, Walcott J, Woods J, Duda J and Merry DE. Expression of expanded repeat androgen receptor produces neurologic disease in transgenic mice. *Hum Mol Genet* 2001;10: 107-116.
[31] Bichelmeier U, Schmidt T, Hubener J, Boy J, Ruttiger L, Habig K, Poths S, Bonin M, Knipper M, Schmidt WJ, Wilbertz J, Wolburg H, Laccone F and Riess O. Nuclear localization of ataxin-3 is required for the manifestation of symptoms in SCA3: in vivo evidence. *J Neurosci* 2007;27: 7418-7428.
[32] De Mees C, Laes J-F, Bakker J, Smitz J, Hennuy B, Van Vooren P, Gabant P, Szpirer J and Szpirer C. Alpha-fetoprotein controls female fertility and prenatal development of the gonadotropin-

releasing hormone pathway through and antiestrogenic action. *Mol Cell Biol* 2006;26: 2012-2018.

[33] Moggs JG, Ashby J, Tinwell H, Lim FL, Moore DJ, Kimber I and Orphanides G. The need to decide if all estrogens are intrinsically similar. *Environ Health Perspect* 2004;112:1137-1142.

[34] Wang T-T, Tavera-Mendoza LE, Laperriere D, Libby E, MacLeod NB, Nagai Y, Bourdeau V, Konstorum A, Lallemant B, Zhang R, Mader S and White JH. Large-scale *in silico* and microarray-based identification of direct 1,25-dihydroxyvitamin D_3 target genes. *Mol Endocrinol* 2005;19:2685-2695.